DOI: 10.1002/ejic.200600772

Catechol-Bearing Dipyrazinylpyridine Complexes of Ruthenium(II)

Fahad A. Al-mutlaq,[a] Pierre G. Potvin,*[a] Athanassios I. Philippopoulos,[b] and Polycarpos Falaras[b]

Keywords: Ruthenium / Tridentate ligands / Photosensitizers / Electron transfer / Energy conversion

The new tridentate ligand 4-(3,4-methylenedioxyphenyl)-2,6-dipyrazinylpyridine (**2**) was prepared in good yield in a one-pot reaction. The Ru^{II} complexes $[Ru(\mathbf{2})_2](PF_6)_2$ and $[Ru(\mathbf{1})(\mathbf{2})](PF_6)_2$ [**1** is 2,6-dipyrazinyl-4-(4-tolyl)pyridine] were prepared in good yields and tested as photosensitizers against $[Ru(\mathbf{1})_2](PF_6)_2$ and $[Ru(ttpy)_2](PF_6)_2$ [ttpy is 4′-(4-tolyl)-2,2′:6′,2′′-terpyridine]. The photosensitization ability follows the order $[Ru(\mathbf{1})_2](PF_6)_2 > [Ru(\mathbf{1})(\mathbf{2})](PF_6)_2 > [Ru(\mathbf{2})_2](PF_6)_2 >> [Ru(ttpy)_2](PF_6)_2$, which is explainable in terms of mechanism and driving force. Hydrolysis of the methylene acetal function affords the catechol-appended complexes $[Ru(\mathbf{3})_2](PF_6)_2$ and $[Ru(\mathbf{1})(\mathbf{3})](PF_6)_2$ [**3** is 4-(3,4-dihydroxyphenyl)-2,6-dipyrazinylpyridine] in excellent yields. These insoluble, paramagnetic precipitates when tested as photosensitizers in homogeneous solution and in one case adsorbed on titania are able to generate photocurrents in a photovoltaic cell, albeit more weakly compared to the so-called N719 dye.

Introduction

Ru^{II} complexes of polypyridine-type ligands continue to enjoy great interest as photosensitizers,[1,2] owing to strong absorption of visible light, favourable redox potentials, appreciable excited state lifetimes and the ability of the excited states to transfer an electron to acceptor molecules or electrodes.[3–5] We have a long-standing interest in discovering non-stereogenic ligands that promote these properties. The present work arises from a desire to incorporate three promising phenomena into the design of a new ligand.

Firstly, we devised sometime ago a new tridentate ligand family with promising features. The first member of the dipyrazinylpyridine (dpp) family of ligands, the 4-*p*-tolyl derivative **1** (Scheme 1), was prepared in a remarkable one-step reaction of commercial materials, in excellent yield and without purification.[6] We have since used this procedure to prepare other dpp examples,[7–9] and extended it to terpyridine synthesis, although those reactions were slower.[9,10] Besides their easier syntheses, the homoleptic Ru^{II} complex $[Ru(\mathbf{1})_2]^{2+}$ revealed an additional advantage of dpp ligands over other tridentates: a longer excited-state lifetime, τ (18 ns at room temperature),[6] compared to that of the analogous terpyridine complex $[Ru(ttpy)_2]^{2+}$ [0.95 ns,[11] ttpy is 4′-(4-tolyl)-2,2′:6′,2′′-terpyridine], a result which can be attributed to the electron-withdrawing effect of the additional nitrogen atoms in stabilizing the ligand π* orbital relative to metal-centred orbitals. At the same time, its absorption (498 nm) and emission (667 nm) were only of slightly lower energy (cf. 490 nm[12] and 640 nm,[11] respectively, for the ttpy analogue), and the shift is the direction favouring the more efficient harvesting of visible light. The $Ru^{III/II}$ oxidation potential was comparatively very high (1.62 V vs. SCE; cf. 1.25 V[13] for the ttpy analogue), again because of the additional nitrogens. This enabled the operation of an electrostatically advantaged reductive quenching mechanism in photosensitization experiments using other dpp complexes.[9]

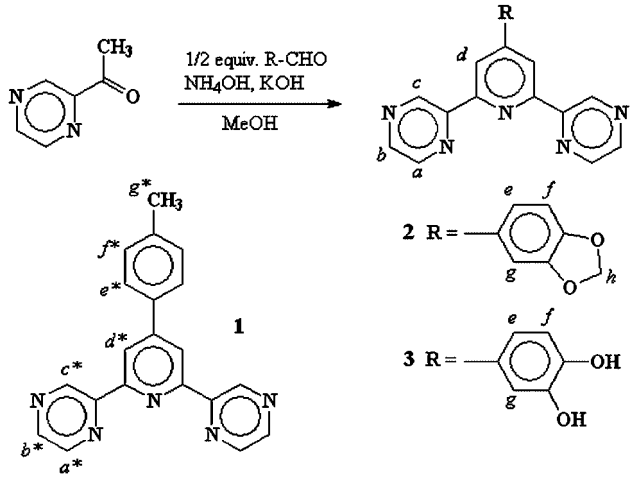

Scheme 1.

Secondly, we recently demonstrated the significant benefit conferred by peripheral carboxylate groups in establishing a binding site for a cationic electron acceptor during oxidative quenching in organic solvents.[14] We wished to

[a] Department of Chemistry, York University, Toronto, ON, Canada M3J 1P3
E-mail: pgpotvin@yorku.ca
[b] Institute of Physical Chemistry, NCSR "Demokritos", Aghia Paraskevi, 15310 Attiki, Greece

gauge the extent of this benefit during reductive quenching with dpp complexes, and to explore the utility of peripheral catecholate groups in supramolecularly binding an electron acceptor.

Thirdly, we knew that catechols form relatively stable complexes with Ti^{IV}.[15–17] As mesoporous TiO_2 is the anchoring substrate for carboxylated Ru^{II} sensitizers on nanocrystalline solar cells,[3] we reasoned that catechol groups would enable stronger, more covalent anchoring to the surface. Indeed, catechol is known to chemisorb to particulate TiO_2[18,19] and Rice et al. have indeed found stronger and faster grafting with catechol-bearing terpyridine complexes on TiO_2-coated electrodes.[20]

Therefore, this paper reports the preparation of a ligand with a dpp core and a peripheral catechol group, the synthesis of its Ru^{II} complexes in both homo- and heteroleptic forms, and an assessment of the photosensitization ability of its Ru^{II} complexes both in solution and while attached to an electrode surface in a photovoltaic cell.

Results

Synthesis

As with the terpyridine analogues,[21] the catechol function was introduced in protected form and deprotected after binding to the metal, this time using the methylene acetal for a less harsh deprotection. As shown in Scheme 1, methylenedioxy ligand **2** was prepared from commercial materials (piperonal, acetylpyrazine and ammonia) in a remarkable one-pot reaction from which it precipitated in good yield (75%, after recrystallization). This compares very favourably with the two-step preparation of the (dimethoxyphenyl)terpyridine analogue in 21–36% overall yield.[21]

The complex $[Ru(\mathbf{2})_2]^{2+}$ was prepared by three procedures with varying results. The direct reaction of $RuCl_3$ with two equiv. of **2** in hot ethylene glycol, followed by isolation of the product by precipitation as the PF_6^- salt using aqueous NH_4PF_6, proceeded in 55–65% yields, but the product contained unacceptable amounts of unidentified impurities. If, instead, the intermediate $Ru(\mathbf{2})Cl_3$ was first prepared in CH_3CN from one equiv. of **2** and $RuCl_3$, then treated with 3 equiv. of $AgBF_4$ to precipitate AgCl and activate the Ru^{III} centre for substitution with a second equiv. of **2** in ethylene glycol, the final $[Ru(\mathbf{2})_2](PF_6)_2$ product was isolated in better yields (65–75%) with less impurity, even though this three-step procedure was more tedious. In a shortened variant, $RuCl_3$ was activated in CH_3CN with 3 equiv. of $AgBF_4$ before reaction with two equiv. of **2** in ethylene glycol, followed by treatment with NH_4PF_6, for a final yield of 75–85% of the purest product yet.

The mixed-ligand species $[Ru(\mathbf{1})(\mathbf{2})]^{2+}$ was also prepared with and without Ag^+ activation.

The $Ru(\mathbf{2})Cl_3$ intermediate was prepared as before, then treated with **1** in ethylene glycol to afford, after the usual work-up, $[Ru(\mathbf{1})(\mathbf{2})](PF_6)_2$ in 45–50% yields, but this product of direct reaction was even less pure than in the homoleptic case. Treatment of $Ru(\mathbf{2})Cl_3$ with 3 equiv. of $AgBF_4$ in ethylene glycol, followed by reaction with one equiv. of **1** in the same solvent and precipitation of the PF_6^- salt, produced $[Ru(\mathbf{1})(\mathbf{2})](PF_6)_2$ in purer form and in better yields (65–70%).

Deprotection of the acetal function proved to be incomplete and slow with plain aqueous acid. Heating with HBr in HOAc afforded complete deprotection in 3–4 d, and proceeded in very high yields (90–95% for $[Ru(\mathbf{3})_2](PF_6)_2$ and 85–90% for $[Ru(\mathbf{1})(\mathbf{3})](PF_6)_2$, after anion exchange with NH_4PF_6).

Despite repeated crystal growth attempts with the four new complexes, only microcrystals or powders were obtained. Upon prolonged standing in CH_3CN solutions, the deprotected salts tended to lose the elements of HPF_6 and form amorphous precipitates that resisted redissolution with heat, but these were easily rescued by redissolving with a small excess of 60% aqueous HPF_6, then diluting with water to re-precipitate the original salts.

Proofs of Identity

^1H NMR spectroscopy was able to verify the identities of the new complexes. While three aromatic signals in free **2** were fortuitously overlapped, they were well separated in the complexes of **2** and **3**. COSY spectra were used in the assignments but, in the heteroleptic cases, many of the signals from one ligand were unfortunately overlapped with the corresponding signals from the other ligand, making individual assignments impossible.

The coordinating nitrogen atoms of heteroaromatic bi- and tridentate ligands are actually in *anti* conformations to minimize dipole–dipole repulsions.[22] Complexation causes a change to *syn* binding conformations and, commonly, the signals adjoining the coordinated nitrogen atoms on the end rings are shifted upfield owing to magnetic anisotropy from the ring current of the perpendicular ligand, while other signals are shifted downfield due to the electron-withdrawing effect of the metal ion. In the present case, the fine doublets due to 5-H and 6-H of the pyrazine rings (which often appeared as broad singlets) were shifted upfield (by 0.8 and 0.3 ppm, respectively) upon complexation, and remained so upon deprotection. However, deprotection predictably caused the disappearance of the distinctive methylene singlets at 6.1–6.2 ppm.

Mass spectrometry confirmed the complex formulations. ES-MS of $[Ru(\mathbf{2})_2]^{2+}$ showed two high-mass clusters, one at *m*/*z* 406 corresponding to the dicationic molecular ion, and a smaller one at *m*/*z* 400 due to partial hydrolysis of the protecting group. With $[Ru(\mathbf{1})(\mathbf{2})]^{2+}$, there was a similar pair of clusters at *m*/*z* 391 and 385. LDI-TOF was used with the deprotected complexes, and both $[Ru(\mathbf{3})_2]^{2+}$ and $[Ru(\mathbf{1})(\mathbf{3})]^{2+}$ showed monocationic molecular ions at *m*/*z* 788 and 769, respectively. While this was the base peak in the former case, a fragment ion dominated the spectrum of the latter (at M-17). In all cases, the mass distributions within each cluster of peaks owing to isotopic diversity was well matched by computed spectra.

Finally, the formulae of all of the new materials were also confirmed by elemental analyses.

UV/Vis Spectroscopy

The UV/Vis spectrum of free **2** showed only n→π* and π→π* transitions in the 200–300 nm range, as is usual with polypyridine-type ligands, but with extended tailing into the visible region. In addition to this same sort of transition, all four complexes showed a similar metal-to-ligand charge transfer (MLCT) band at λ_{max} 500–502 nm (Table 1), as well as a much smaller feature near 405 nm. The MLCT bands were typical of complexes of this type and virtually the same as that of the analogous $[Ru(\mathbf{1})_2]^{2+}$.[6] The influence of the oxygen functionalities is apparently weak, shifting the peak positions only slightly toward the red, in agreement with their π-donating character. The only significant difference between them was that the catechol forms were more strongly absorbing than were the protected forms, with a molar extinction coefficient (ε) value 37% larger with one catechol unit, and 53% larger with two. The terpyridine analogues[21] behaved differently in that deprotection to the catechol forms caused 8 nm red shifts in λ_{max} and much larger increases in ε (by 133% and 57% for homo- and heteroleptic varieties, respectively) than with our complexes.

We also explored the effect of deprotonation of the catechol units on the MLCT transitions, using sample solutions of the two deprotected complexes prepared at various [Et_3N]:[Ru] ratios in CH_3CN. The effect was mild: the red color of the pure complexes changed to a light brown, as the MLCT λ_{max} drifted slightly with $[Ru(\mathbf{3})_2]^{2+}$ (from 502 to 506 nm with 0–6 equiv. of Et_3N) but held steady at 500 nm with $[Ru(\mathbf{1})(\mathbf{3})]^{2+}$ (with 0–4 equiv. of base), while the band tails lengthened toward the red and the ε values at λ_{max} decreased gently in lock-step with increasing [Et_3N]:[Ru].

Cyclic Voltammetry

Cyclic voltammograms were obtained for all four complexes in degassed CH_3CN and DMF (Figure 1 is representative). Oxidation was only detected in CH_3CN but was irreversible in all cases. Limited-range scans did not improve the reversibility. Some of the features in the negative range appeared only after first scanning positive, so were probably reductions of oxidation products having undergone subsequent chemical transformations. Therefore DPV scans were employed to help determine $E_{1/2}$ values. Except for more positive potentials owing to the electron-poorer pyrazine rings, the results (Table 1) mimicked the behaviour

Table 1. Spectroscopic, electrochemical and photochemical data in CH_3CN solutions.

Complex	λ_{max}, nm [ε, 10^4 M^{-1} cm^{-1}]	$E_{1/2}(Ru^{III/II})$[a] V vs. SCE	$E_{1/2}(L^{+/0})$ V vs. SCE	$E_{1/2}(L^{0/-})$ V vs. SCE	k_f 10^{-5} s^{-1}
$[Ru(\mathbf{2})_2]^{2+}$	502 (1.65)	1.56	1.85	–0.86	4.68(6)
$[Ru(\mathbf{1})(\mathbf{2})]^{2+}$	500 (1.53)	1.60	1.70	–0.77	4.82(5)
$[Ru(\mathbf{3})_2]^{2+}$	502 (2.52)	(1.80)	1.34	–0.80	–
$[Ru(\mathbf{1})(\mathbf{3})]^{2+}$	500 (2.09)	1.65	–	–0.85	–
$[Ru(\mathbf{1})_2]^{2+}$ [6]	498 (1.66)	1.62	–	–0.85	8.9(5)[b]
$[Ru(ttpy)_2]^{2+}$	490 (1.55)[12]	1.25[13]	–	–1.24[13]	0.936(4)[23]

[a] In parentheses, E_{pa}. [b] This work.

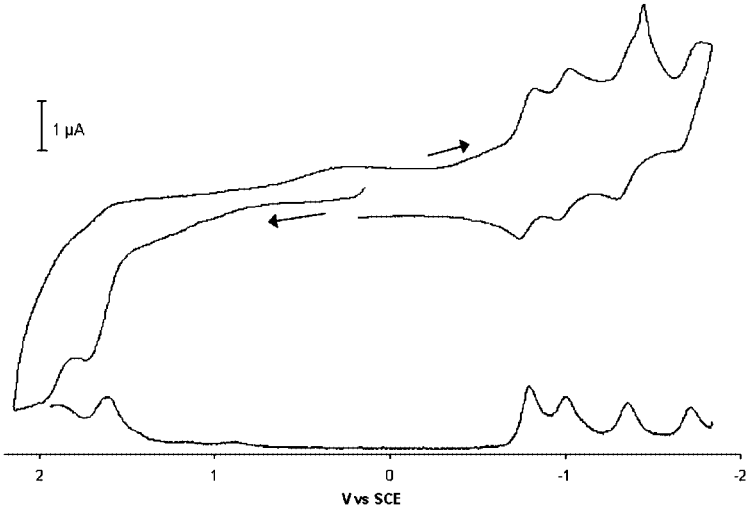

Figure 1. Cyclic voltammogram (upper plot) and differential pulse voltammogram (DPV, lower plot) of $[Ru(\mathbf{1})_2](PF_6)_2$ in CH_3CN containing 0.1 M Bu_4NPF_6.

of the terpyridine analogues,[21] in that metal oxidation was followed by a more positive ligand oxidation when in protected form, and a less positive one after deprotection to catechol forms. Both metal oxidation and first ligand reduction potentials occurred near those previously measured for the dpp complex $[Ru(\mathbf{1})_2]^{2+}$ lacking a catechol unit,[6] and up to three further reduction waves occurred at 100–340 mV intervals.

Photosensitization

Samples of all four new complexes were submitted to the assessment protocol[23] that we have used several times to gauge photosensitizer ability[9,12,14,24,25] by monitoring the rate of accumulation of the methyl viologen cation radical ($MV^{\cdot+}$) arising by electron transfer from the photo-excited state to methyl viologen (MV^{2+}) in the presence of a sacrificial reductant, triethanolamine (TEOA), which is used to reduce the Ru^{III} photoproduct back to the starting Ru^{II} state. When a mixture of $[Ru(\mathbf{3})_2]^{2+}$, $MV(PF_6)_2$ and TEOA in CH_3CN was irradiated at 400–600 nm, the Ru complex quantitatively formed a dark precipitate and very little $MV^{\cdot+}$ accumulated in the supernatant, as judged by the absorption spectrum. This precipitation recurred with repeated trials. The precipitate was isolated by filtration, but the material was insoluble in most solvents, including CH_3CN and DMF. It was soluble in TFA, but it was NMR-silent in [D]TFA, suggesting that it was paramagnetic. Its LDI-TOF mass spectrum was very noisy and generally uninformative, showing very few peaks and these were not attributable to any reasonable formulation. No further characterization was carried out, but control experiments revealed that the three chemical components, the Ru^{II} complex, MV^{2+} and TEOA, were all required to produce the precipitation. We also found that no precipitation occurred in the dark; light – even sunlight through a window – was required. This precipitation behaviour was also noted with $[Ru(\mathbf{1})(\mathbf{3})]^{2+}$, but we did not carry out control experiments in that case.

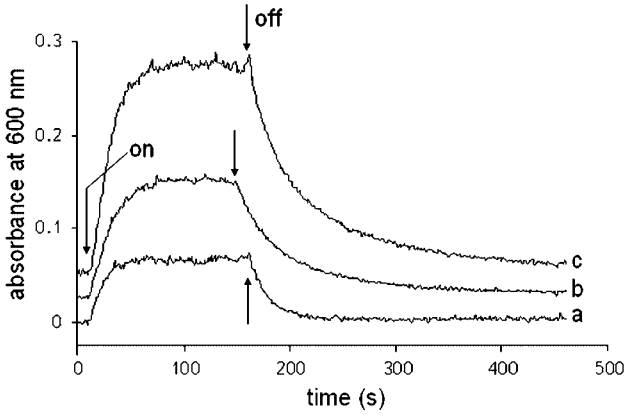

Figure 2. Plots of absorbance at 600 nm over time for (a) $[Ru(\mathbf{3})_2]^{2+}$, (b) $[Ru(\mathbf{1})(\mathbf{3})]^{2+}$, offset by 0.025 absorbance units, and (c) $[Ru(\mathbf{1})_2]^{2+}$, offset by 0.05 absorbance units. Arrows indicate the start and end of irradiation.

In contrast, the protected forms, $[Ru(\mathbf{2})_2]^{2+}$and $[Ru(\mathbf{1})(\mathbf{2})]^{2+}$, behaved normally, showing the same pattern as had been seen with other sensitizers (Figure 2): a rapid, steady rise in absorbance at 600 nm owing to $MV^{\cdot+}$, followed by a levelling off and, after turning off the light, a slow aerobic decay back to the starting absorbance. For comparison, $[Ru(\mathbf{1})_2]^{2+}$ was assessed in the same manner. The data were treated as before,[23] and the first-order rate constants k_f for $MV^{\cdot+}$ accumulation are reported in Table 1. These clearly show that all three species were significantly better sensitizers than was the terpyridine complex $[Ru(ttpy)_2]^{2+}$, and that $[Ru(\mathbf{1})_2]^{2+}$ was a better sensitizer than the catechol-containing species.

Photovoltaic Performance

A photovoltaic cell was assembled for each of the two catechol-bearing complexes. The sensitizer was adsorbed from a CH_3CN solution onto a titania-coated conductive glass plate. A solid-state electrolyte film was sandwiched between this and a platinized counter-electrode. The current and potential between the electrodes were monitored while the assembly was irradiated using a "standard" light source approximating the sun's spectrum and density (per unit area) at the Earth's surface. Another assembly was similarly prepared using the so-called N719 dye, the bis(tetrabutylammonium) salt of *cis*-bis(2,2′-bipyridyl-4,4′-dicarboxylic acid)bis(thiocyanato)ruthenium(II), to serve as a comparison. The results are presented in Table 2 in terms of the four quantities of importance for solar cells: the open-circuit potential V_{oc}, the short-circuit current density I_{sc}, the "fill factor" (*FF*), which is the maximum or peak power ($V \times I$) divided by V_{oc} and by I_{sc}, and the photon-to-electron conversion efficiency η.

Table 2. Photovoltaic characteristics.

Sensitizer	I_{sc} [mA cm^{-2}]	V_{oc} [mV]	*FF*	η [%]
$[Ru(\mathbf{3})_2]^{2+}$	0.297	337	0.52	0.05
$[Ru(\mathbf{1})(\mathbf{3})]^{2+}$	1.006	348	0.52	0.19
N719	9.29	583	0.53	2.87

Gratifyingly, the new catechol dyes both were able to generate a current when irradiated under these conditions. However, they showed significantly lower efficiencies (η) than the well studied N719 dye, which generated a stronger V_{oc} and a much larger I_{sc} under the same conditions, while *FF* was virtually the same for all three sensitizers. Interestingly, it appears that the asymmetric catechol complex is about four times more efficient than the symmetrical bis(catechol) one, in spite of the latter's ability to absorb more light (higher ε). Two catechol-bearing terpyridine complexes have previously been tested in photovoltaic cells, with moderately good results.[20] The cell constitution was different in that a liquid electrolyte was used, and the results are not directly comparable to ours, but the η values were also

significantly lower than for carboxylated sensitizers like the N719 dye, in spite of the determination that the surface grafting was superior and faster with catechol than with carboxylate groups.

Discussion

The weak base-dependence of the position and intensity of the MLCT absorption of the two catechol-bearing complexes, and the similarity in the $E_{1/2}(Ru^{II/I})$ values of all dpp complexes is consistent with the LUMO in dpp complexes being centred over a pyrazine ring. This is reasonable, since pyrazine rings are the most electron-poor and are π-disconnected from each other and from the 4-substituent on the central pyridine ring. Moreover, pyrazine rings on the less π-rich ligand **1** are expected to be of lower energy than those of the oxygenated **2** or **3**. In contrast, the LUMO of a tpy ligand is likely centred over the central pyridine ring, more strongly influenced, therefore, by a 4′-substituent on that ring, as demonstrated by the MLCT absorptions of the tpy analogues.[21]

According to its very positive $E_{1/2}(Ru^{III/II})$ value, $[Ru(\mathbf{1})_2]^{2+}$ can undergo reductive quenching, and the other dpp complexes should also have been capable of reductive quenching. However, they would not benefit from the same driving force. In comparison with the *p*-tolyl groups in $[Ru(\mathbf{1})_2]^{2+}$, the methylenedioxy group in **2** is much more strongly electron-donating in character. Since electron-donating substituents destabilize the metal-centered orbitals to a greater degree than they destabilize the pyrazine-centered LUMO, and especially since the electron-donating substituents are π-disconnected from the pyrazines, $E(Ru^{III/II})$ should be much more affected than $E(Ru^{II/I})$ and shifted to less positive values. Consequently, both absorption and emission (and E_{00}) will shift to lower energies, as the gaps between the ground state and ^{1}MLCT or ^{3}MLCT states become narrower as a result. Since both $E(Ru^{III/II})$ and E_{00} will be depressed by the same HOMO destabilization, $E(Ru^{III/II*}) = E(Ru^{III/II}) - E_{00}$ will be little changed and oxidative quenching will remain impossible. However, $E(Ru^{II*/I}) = E_{00} + E(Ru^{II/I})$ will decrease. While this decrease may not be sufficient to prevent reductive quenching from occurring, it will certainly reduce the driving force for the initial reaction of the excited state with TEOA. According to Marcus–Hush theory, that driving force determines the rate of the electron transfer reaction.[26] This then explains the stronger photosensitization in the order $[Ru(\mathbf{1})_2]^{2+} > [Ru(\mathbf{1})(\mathbf{2})]^{2+} > [Ru(\mathbf{2})_2]^{2+}$.

Yet all three dpp complexes were better than $[Ru(ttpy)_2]^{2+}$. We can identify two reasons for this. Firstly, we can expect enhanced steady-state concentrations of the excited states with dpp sensitizers, owing to three factors: the absorption bands are more centred in the 400–600 nm irradiation window, there is increased light absorption (higher ε values) and, because $[Ru(\mathbf{1})_2]^{2+}$ was previously found to have a higher τ value than had $[Ru(ttpy)_2]^{2+}$, as mentioned earlier, it is reasonable to expect similarly higher values for the other dpp complexes. Secondly, and perhaps most importantly, the dpp-containing complexes are expected to follow a reductive quenching mechanism while $[Ru(ttpy)_2]^{2+}$ can only undergo oxidative quenching. As the crucial step involves a reaction of the excited state with the neutral TEOA in reductive quenching, or with the dicationic MV^{2+} during oxidative quenching, reductive quenching is electrostatically advantaged.

In light of this, we can postulate a reason for precipitate formation during irradiation of the complexes of **3**. With the additional nitrogens present, catechol oxidation would have occurred at a slightly more positive potential with these than that measured for the *tpy* analogues (1.21 V vs. SCE),[21] but this would probably still remain below $E(Ru^{III/II})$ (as exemplified by the *p*-tolyl case). However, under the basic conditions provided by TEOA, the catechol groups had probably ionized – even more likely because of the additional nitrogens – since this would have served to balance the metal charge and would have constituted a binding site for MV^{2+}. The catecholate oxidation would then have occurred at a less positive potential. It is therefore probable that catecholate groups served as internal quenchers of the excited states of our deprotected complexes. This is illustrated in Scheme 2, where a possible mechanism for precipitate formation is compared to "normal" photo-catalytic cycles. Just as with other Ru^{II} complexes of this type, the ^{3}MLCT excited state **B** can undergo "normal" non-radiative decay (path *a*). In our case, it can also undergo non-radiative decay from an internally quenched state **D** (path *b*), or "normal" reductive quenching by TEOA to **C** followed by electron transfer to MV^{2+} and regenerating the ground state **A** (path *c*). Alternatively, the internally quenched state **D** can feasibly be reduced by TEOA to **C** in an "abnormal" reductive quenching (path *d*), or oxidized by MV^{2+} (path *e*) in "abnormal" oxidative quenching to produce a radical product **E**. But $E(TEOA^{\cdot+/0})$ is 0.81 V vs. SCE,[27] i.e. below the catechol oxidation potential. Hence, as depicted, **D** should have been able to oxidize TEOA and path *d* should have been followed. At the same time, oxidative quenching of **D** (path *e*) might also have occurred and the cation radical product **E** should have been reduced by TEOA to regenerate **A** (path *f*). In both cases, $MV^{\cdot+}$ would have accumulated and no insoluble paramagnetic species should have formed by path *g*.

With TEOA acting as a base instead, catecholates would result. If their lower oxidation potentials indeed lie below $E(TEOA^{\cdot+/0})$, then paths *d* and *f* would be obviated and **E** would accumulate by path *e*. (The amount of $MV^{\cdot+}$ so formed could not have exceeded the amount of Ru complex initially present; it would have been too small to observe and would have quickly decayed aerobically.) The fates of the resulting radicals **E** are unknown, but deprotonation (by TEOA) and dimerization by phenolic coupling are likely outcomes, eventually resulting in the paramagnetic precipitates that were observed.

There are several possible reasons for the better photovoltaic behaviour of the N719 dye. Its MLCT band at 534 nm extends well beyond 700 nm,[28] although the ε

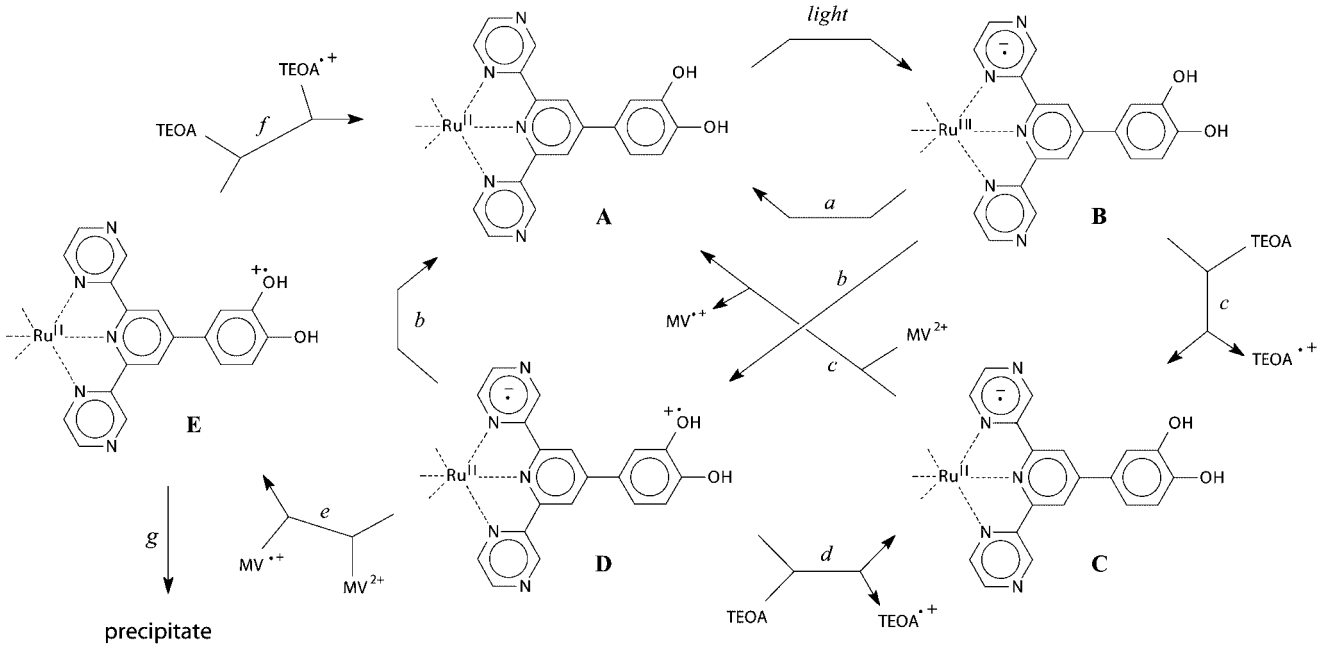

Scheme 2.

value at λ_{max} is actually a little weaker (1.42×10^4 M^{-1} cm^{-1}) than with our materials. Its τ value (50 ns)[28] is also larger than that of $[Ru(\mathbf{1})_2]^{2+}$. Photovoltaic sensitizers normally have $E(Ru^{III/II})$ well below 1 V vs. SCE (0.85 V for N719 itself,[28] 0.61 V[29] for $[Ru(tpy)(SCN)_3]^0$), much less positive than in dpp complexes, so that the driving force for electron injection is much weaker with dpp complexes. Internal quenching by catechol groups could short-circuit the photoconduction process by constituting a second, "abnormal", non-radiative decay path (path *b* in Scheme 2) for the excited state, and thereby decrease the solar conversion efficiency. This would need to occur at a rate competitive with electron injection, but the literature suggests that electron injection is exceedingly fast (on sub-ps or even fs timescales)[30–32] and it occurs even with sensitizers having exceedingly short τ values.[33]

Finally, another contributing factor may have been the state of aggregation on the surface. In multilayer assemblies, the outer layers may be too distant from the surface for an efficient photo-induced transfer of an electron to the surface, and may insulate the inner layers from the I^-/I_3^- of the bulk phase, preventing the photo-produced Ru^{III} state from returning to the ground Ru^{II} state, and thereby effectively slowing down or stopping the catalytic cycle. Rice et al. report using cholic acid derivatives to inhibit aggregation,[20] but no such treatment was applied in our experiments.

Overall, the differences in photovoltaic behaviour between the three complexes tested may be due to a combination of factors, including differences in the complexes' photophysical properties once anchored to the electrode surface, the driving force for electron injection and the state of aggregation at the surface. It may be possible to address each of these factors in new sensitizer designs.

Experimental Section

General: Samples of **1** and $[Ru(\mathbf{1})_2](PF_6)_2$ were prepared according to Liegghio et al.[6]

All NMR spectra were obtained with a Bruker AMX-400 spectrometer at 300 K. Signal assignments are given using the position labels of Scheme 1. Electron-impact mass spectrometry (EI-MS) was performed by Dr. Alex Young of the University of Toronto on a Micromass 70S-250 sector instrument at 70 eV. Laser Desorption Ionization-Time of Flight mass spectra (LDI-TOF-MS) were obtained on a Voyager DE STR instrument, while electrospray mass spectra were obtained on a Sciex-TAGA 600E instrument. Elemental analyses were performed by Guelph Chemical Laboratories, Guelph, ON, Canada.

Electronic spectroscopy was performed on a HP 8452A instrument. Stock solutions that were 5×10^{-4} M in Ru were prepared. Aliquots (0.5 mL) were diluted with 2 mL of CH_3CN in a disposable polymethacrylate cuvette (spectral range: 275–800 nm) to achieve a final concentration of 1×10^{-4} M. Acetonitrile in a matching cuvette was used for baseline correction. The cuvettes were maintained at 25 °C by a Peltier block controlled by a HP 89090A controller. To explore the effect of deprotonation, 2 mL aliquots of the Ru stock were combined with 0–2 mL of an 8×10^{-4} M stock solution of Et_3N in CH_3CN, and the resulting mixture was diluted to 4 mL with CH_3CN. Samples were also prepared with 2.25–3 mL Et_3N without further dilution, and the increased volume was taken into account. The position of the MLCT λ_{max} was monitored and the nominal ε values were computed.

Cyclic voltammetry was performed with an Obbligato Objectives Faraday MP potentiometer, using a graphite working electrode, a Pt wire counter electrode, and a Ag/AgCl *quasi*-reference electrode, which was prepared by immersing a virgin Ag wire in 1 M HCl and rinsing with H_2O and absolute ethanol. Sample solutions in either CH_3CN or DMF were assembled by combining 5 mL of a 5×10^{-3} M Ru stock solution and 5 mL of a 0.1 M stock solution of tetrabutylammonium hexafluorophosphate (TBAH), then degassed

by bubbling with Ar for 2–3 min. For the last scan at the end of an experiment, 5 mL of a 5×10^{-3} M ferrocene (Fc, $E°$ = 0.40 V in CH_3CN containing TBAH vs. SCE)[34] stock solution was added.

For photosensitizer assessments, the equipment, sample preparation, data acquisition and data treatment were exactly as described earlier.[23]

For the photovoltaic measurements, titania films were prepared on commercial Pilkington TEC 8 conductive glass plates according to a standard procedure,[28,35] using the scalpel technique. The films were sintered and stored in a dessicator in the dark. Before impregnating the films, they were heat-treated at 450 °C for 30 min. While still hot at ca. 100 °C, they were immersed in sensitizer solutions, where they remained for grafting for 3 d. The sensitizers were dissolved in dry acetonitrile (distilled over P_2O_5) giving a ca. 1×10^{-4} M solution of $[Ru(\mathbf{3})_2](PF_6)_2$ and a ca. 2×10^{-4} M solution of $[Ru(\mathbf{1})(\mathbf{3})](PF_6)_2$, both of which were stored in the dark. A solid-state polyethylene oxide/titania/I^-/I_3^- composite electrolyte[36,37] was used in the course of the experiments. The electrolyte was sandwiched between the photoelectrode and the platinized counterelectrode. Current–voltage (I–V) characteristics were obtained by connecting the cell to a variable resistor together with a micro-amperemeter in series and a voltmeter in parallel. Illumination was provided by a 300-W Xe light source (Oriel). A cut-off filter was used to exclude wavelengths less than 400 nm so as to prevent the generation of electron-hole pairs through direct TiO_2 bandgap excitation. Through accurate positioning of the cell assembly, all measurements were obtained under global air mass 1.5 (AM 1.5) solar irradiation conditions[38] (power density 1000 W m^{-2}). The experiments were repeated four times for each complex and a mean value was taken. *cis*-Bis(2,2′-bipyridyl-4,4′-dicarboxylato)bis(thiocyanato)ruthenium(II) bis(tetrabutylammonium) salt (N719 dye), purchased from Solaronix s.a., was used for comparison.

4-(3,4-Methylenedioxyphenyl)-2,6-dipyrazinylpyridine (2): Acetylpyrazine (0.20 g, 1.6 mmol) and piperonal (0.12 g, 0.8 mmol) were dissolved in a mixture of concentrated NH_4OH (0.5 mL), 15% aq. KOH (5.2 mL), and methanol (5.7 mL), giving a canary yellow solution. The mixture turned beige over a period of 4 d at room temperature, and had formed a precipitate. This was isolated by filtration, rinsing with MeOH/H_2O (1:1), then heated in hot acetone for 3 h to dissolve. The solution was cooled, then filtered. The solid was washed with acetone and ether, and then left to dry in a 70–80 °C oven, providing **2** in 75% yield (0.28 g). ^{1}H NMR (400 MHz, $CDCl_3$, 300 K): δ = 9.90 (s, 1 H, *c*), 8.73 (3s, 3 H, *a*, *b* & *d*), 7.39 (d, 1 H, *e*), 7.28 (s, 1 H, *g*), 6.99 (d, 1 H, *f*), 6.09 (s, 2 H, *h*) ppm. EI–MS: *m*/*z* = 355. $C_{20}H_{13}N_5O_2$ (355.4): calcd. C 67.60, H 3.70, N 19.71; found C 67.54, H 3.75, N 19.58.

$[Ru(\mathbf{2})_2](PF_6)_2$: $RuCl_3 \cdot 3H_2O$ (0.10 g, 0.38 mmol) and $AgBF_4$ (0.20 g, 1.2 mmol) were heated in acetonitrile at reflux for 3 h, then filtered free of AgCl, affording a deep green solution. The solvent was then removed and replaced with fresh ethylene glycol. Ligand 2 (0.28 g, 0.76 mmol) was added, and the mixture was heated to reflux overnight, changing to a deep red colour. The Ru complex was precipitated by adding two equivalents of aqueous NH_4PF_6 (0.12 g, 0.76 mmol), collected by filtration, rinsed with ether and left to dry overnight in a 60–80 °C oven. Yield 0.94 g (85%). ^{1}H NMR (400 MHz, CD_3CN, 300 K): δ = 9.76 (s, 2 H, c), 9.13 (s, 2 H, d), 8.40 (d, 2 H, b), 7.82 (d, 1 H, e), 7.78 (s, 1 H, g), 7.54 (d, 2 H, a), 7.27 (d, 1 H, f), 6.23 (s, 2 H, h) ppm. ES-MS: m/z = 406. $C_{40}H_{26}N_{10}O_4Ru^{2+}$ requires 406. $C_{40}H_{26}F_{12}N_{10}O_4P_2Ru$ (1101.7): calcd. C 43.61, H 2.38, N 12.71; found C 43.96, H 2.29, N 12.69.

$[Ru(\mathbf{1})(\mathbf{2})](PF_6)_2$: $RuCl_3 \cdot 3H_2O$ (0.10 g, 0.38 mmol) and ligand **2** (0.14 g, 0.38 mmol) were dissolved in acetonitrile and the mixture was left to reflux for 3 h, whence the reaction mixture became deep brown. Then, $AgBF_4$ (0.2 g, 1.2 mmol) was added, and heating continued for an additional 3 h, developing a deep green colour. This mixture was filtered free of AgCl, the filtrate was freed of solvent, then diluted with fresh ethylene glycol. Ligand **1** (0.12 g, 0.38 mmol) was then added and the mixture was heated to reflux overnight, changing to a deep red. The complex was precipitated by addition of aqueous NH_4PF_6 (0.12 g, 0.76 mmol), collected by filtration, and washed with diethyl ether, then left to dry overnight in a 60–80 °C oven. Yield 0.75 g (70%). ^{1}H NMR (400 MHz, CD_3CN, 300 K): δ = 9.76 (2s, 2 H, *c* & *c**), 9.19 (s, 1 H, *d*), 9.12 (s, 1 H, *d**), 8.40 (m, 2 H, *b* & *b**), 8.17 (d, 2 H, *e**), 7.82 (d, 1 H, *e*), 7.78 (s, 1 H, *g*), 7.66 (d, 2 H, *f**), 7.55 (m, 2 H, *a* & *a**), 7.27 (d, 1 H, *f*), 6.23 (s, 1 H, *h*), 2.58 (s, 3 H, *g**) ppm. ES-MS: *m*/*z* = 391.0. $C_{40}H_{28}N_{10}O_2Ru^{2+}$ calcd. 390.9. $C_{40}H_{28}F_{12}N_{10}O_2P_2Ru$ (1071.7): calcd. C 44.83, H 2.63, N 13.07; found C 44.67, H 2.54, N 12.96.

$[Ru(\mathbf{3})_2](PF_6)_2$: $[Ru(\mathbf{2})_2](PF_6)_2$ (0.10 g, 0.91 mmol) was dissolved in 30–45% HBr in acetic acid (40 mL) and heated to just below reflux temperature for 3–4 d, whence the colour turned deep brown. The solvent was removed in vacuo and the residue was dissolved in a minimal amount of CH_3CN. The product was precipitated with 2 M aqueous NH_4PF_6 (30 mL), collected by filtration and washed with diethyl ether, then was left to dry overnight in a 50–60 °C oven. Yield 1.02 g (95%). ^{1}H NMR (400 MHz, CD_3CN, 300 K): δ = 9.77 (s, 2 H, *c*), 9.13 (s, 2 H, *d*), 8.38 (d, 2 H, *b*), 7.79 (s, 2 H, *g*), 7.70 (d, 1 H, *e*), 7.54 (d, 2 H, *a*), 7.22 (d, 1 H, *f*) ppm. LDI-TOF-MS: *m*/*z* = 788.1. $C_{40}H_{28}N_{10}O_2Ru^+$ requires 788.1. $C_{38}H_{26}N_{10}O_4P_2F_{12}Ru$ (1077.7): calcd. C 43.65, H 2.51, N 13.40; found C 43.47, H 2.43, N 13.36.

$[Ru(\mathbf{1})(\mathbf{3})](PF_6)_2$: The procedure used to generate $[Ru(\mathbf{3})_2](PF_6)_2$ was applied to $[Ru(\mathbf{1})(\mathbf{2})](PF_6)_2$ (0.10 g, 0.93 mmol). Yield 0.95 g (90%). ^{1}H NMR (400 MHz, CD_3CN, 300 K): δ = 9.79 (2s, 2 H, *c* & *c**), 9.19 (2s, 2 H, *d* & *d**), 8.39 (m, 2 H, *b* & *b**), 8.17 (d, 2 H, *e**), 7.87 (s, 1 H, *g*), 7.71 (d, 1 H, *e*), 7.64 (d, 2 H, *f**), 7.53 (m, 2 H, *a* & *a**), 7.22 (d, 1 H, *f*), 2.58 (s, 3 H, *g**) ppm. LDI-TOF-MS: *m*/*z* = 768.7. $C_{39}H_{27}N_{10}O_2Ru^+$ requires 768.3. $C_{39}H_{27}N_{10}O_2P_2F_{12}Ru$ (1058.7): calcd. C 44.25, H 2.57, N 13.23; found C 44.14, H 2.51, N 13.19.

Acknowledgments

F. A. and P. G. P. thank the Natural Sciences and Engineering Research Council of Canada for financial support.

[1] V. Balzani, P. Ceroni, B. Ferrer, *Pure Appl. Chem.* **2004**, *76*, 1887–1901.
[2] A. Islam, H. Sugihara, H. J. Arakawa, *Photochem. Photobiol. A* **2003**, *158*, 131–138.
[3] M. Grätzel, *Pure Appl. Chem.* **2001**, *73*, 459.
[4] C. Klein, M. K. Nazeeruddin, P. Liska, D. Di Censo, N. Hirata, E. Palomares, J. R. Durrant, M. Grätzel, *Inorg. Chem.* **2005**, *44*, 178–180.
[5] P. Wang, C. Klein, R. Humphry-Baker, S. M. Zakeeruddin, M. Grätzel, *J. Am. Chem. Soc.* **2005**, *127*, 808–809.
[6] R. Liegghio, P. G. Potvin, A. B. P. Lever, *Inorg. Chem.* **2001**, *40*, 5485.
[7] T. Manivannan, P. G. Potvin, manuscript in preparation.
[8] M. Abboud, P. G. Potvin, manuscript in preparation.
[9] S. Vaduvescu, P. G. Potvin, *Eur. J. Inorg. Chem.* **2004**, 1763–1769.
[10] S. Vaduvescu, P. G. Potvin, *Acta Crystallogr., Sect. E* **2003**, *59*, o483–484.

[11] F. Barigelletti, L. Flamigni, V. Balzani, J.-P. Collin, J.-P. Sauvage, A. Sour, E. C. Constable, A. M. W. Cargill Thompson, *J. Chem. Soc., Chem. Commun.* **1993**, 942.
[12] C. Mikel, P. G. Potvin, *Polyhedron* **2002**, *21*, 49.
[13] K. Kalyanasundaram, M. K. Nazeeruddin, M. Grätzel, G. Viscardi, P. Savarino, E. Barini, *Inorg. Chim. Acta* **1992**, *198*, 831.
[14] P. G. Potvin, P. U. Luyen, J. Bräckow, *J. Am. Chem. Soc.* **2003**, *125*, 4894–4906.
[15] B. A. Borgias, S. R. Cooper, Y. B. Koh, K. N. Raymond, *Inorg. Chem.* **1984**, *23*, 1009–1016.
[16] K. Gigant, A. Rammal, M. Henry, *J. Am. Chem. Soc.* **2001**, *123*, 11632–11637.
[17] M. Albrecht, M. Napp, M. Schneider, P. Weis, R. Fröhlich, *Chem. Eur. J.* **2001**, *7*, 3966–3975.
[18] R. Rodriguez, M. A. Blesa, A. E. Regazzoni, *J. Colloid Interface Sci.* **1996**, *177*, 122–131.
[19] P. A. Connor, K. D. Dobson, A. J. McQuillan, *Langmuir* **1995**, *11*, 4193–4195.
[20] C. R. Rice, M. D. Ward, M. K. Nazeeruddin, M. Grätzel, *New J. Chem.* **2000**, *24*, 651–652.
[21] B. Whittle, N. S. Everest, C. Howard, M. D. Ward, *Inorg. Chem.* **1995**, *34*, 2025–2032.
[22] J. Zadykowicz, P. G. Potvin, *J. Coord. Chem.* **1999**, *47*, 395–407.
[23] P. G. Potvin, P. U. Luyen, F. A. Al-mutlaq, *New J. Chem.* **2001**, *25*, 839.
[24] C. M. Chamchoumis, P. G. Potvin, *Inorg. Chim. Acta* **2001**, *325*, 1–8.
[25] F. A. Al-mutlaq, P. G. Potvin, *J. Combin. Chem.* **2005**, in press.
[26] R. A. Marcus, N. Sutin, *Biochim. Biophys. Acta* **1985**, *811*, 265.
[27] K. Tokumaru, *J. Porphyrins Phthalocyanines* **2001**, *5*, 77–86.
[28] M. K. Nazeeruddin, A. Kay, I. Rodicio, R. Humphry-Baker, E. Muller, P. Liska, N. Vlachopoulos, M. Grätzel, *J. Am. Chem. Soc.* **1993**, *115*, 6382–6390.
[29] M. K. Nazeeruddin, P. Pechy, T. Renouard, S. M. Zakeeruddin, R. Humphry-Baker, P. Comte, P. Liska, L. Cevey, E. Costa, V. Shklover, L. Spiccia, G. B. Deacon, C. A. Bignozzi, M. Grätzel, *J. Am. Chem. Soc.* **2001**, *123*, 1613–1624.
[30] R. Eichberger, F. Willig, *Chem. Phys.* **1990**, *141*, 159–173.
[31] J. M. Rehm, G. L. McLendon, Y. Nagasawa, K. Yoshihara, J. Moser, M. Grätzel, *J. Phys. Chem.* **1996**, *100*, 9577–9578.
[32] Y. Tachibana, J.-E. Moser, M. Grätzel, D. R. Klug, J. R. Durrant, *J. Phys. Chem.* **1996**, *100*, 20056–20062.
[33] S. Ferrere, B. A. Gregg, *J. Am. Chem. Soc.* **1998**, *120*, 843–844.
[34] N. G. Connelly, W. E. Geiger, *Chem. Rev.* **1996**, *96*, 877.
[35] I. M. Arabatzis, T. Stergiopoulos, G. Katsaros, M. C. Bernard, D. Labou, S. G. Neofytides, P. Falaras, *Appl. Catal. B* **2003**, *42*, 187–201.
[36] G. Katsaros, T. Stergiopoulos, I. M. Arabatzis, K. G. Papdokostaki, P. Falaras, *J. Photochem. Photobiol. A* **2002**, *149*, 191–198.
[37] T. Stergiopoulos, G. Arabatzis, P. Katsaros, P. Falaras, *Nano Lett.* **2002**, *2*, 1259–1261.
[38] R. Hulstrom, R. Bird, C. Riordan, *Solar Cells* **1985**, *15*, 365–391.

Received: August 18, 2006
Published Online: April 11, 2007

